Published in final edited form as:
Dev Biol. 2014 February 1; 386(1): 1–11. doi:10.1016/j.ydbio.2013.12.014.

Coordinated activity of Spry1 and Spry2 is required for normal development of the external genitalia

Saunders T. Ching[1,2], **Gerald R. Cunha**[2], **Laurence S. Baskin**[2], **M. Albert Basson**[3], and **Ophir D. Klein**[1,4,5,6]

[1]Department of Orofacial Sciences, University of California, San Francisco

[2]Department of Urology, University of California, San Francisco

[3]Department of Craniofacial Development and Stem Cell Biology, King's College, London

[4]Program in Craniofacial and Mesenchymal Biology, University of California, San Francisco

[5]Institute for Human Genetics, University of California, San Francisco

[6]Department of Pediatrics, University of California, San Francisco

Abstract

Development of the mammalian external genitalia is controlled by a network of signaling molecules and transcription factors. Because FGF signaling plays a central role in this complicated morphogenetic process, we investigated the role of Sprouty genes, which are important intracellular modulators of FGF signaling, during embryonic development of the external genitalia in mice. We found that Sprouty genes are expressed by the urethral epithelium during embryogenesis, and that they have a critical function during urethral canalization and fusion. Development of the genital tubercle (GT), the anlage to the prepuce and glans penis in males and glans clitoris in females, was severely affected in male embryos carrying null alleles of both *Spry1* and *Spry2*. In *Spry1*$^{-/-}$;*Spry2*$^{-/-}$ embryos, the internal tubular urethra was absent, and urothelial morphology and organization was abnormal. These effects were due, in part, to elevated levels of epithelial cell proliferation in *Spry1*$^{-/-}$;*Spry2*$^{-/-}$ embryos. Despite changes in overall organization, terminal differentiation of the urothelium was not significantly affected. Characterization of the molecular pathways that regulate normal GT development confirmed that deletion of Sprouty genes leads to elevated FGF signaling, whereas levels of signaling in other cascades were largely preserved. Together, these results show that levels of FGF signaling must be tightly regulated during embryonic development of the external genitalia in mice, and that this regulation is mediated in part through the activity of Sprouty gene products.

Keywords

Genital tubercle; Sprouty; FGF; urethra; hypospadias

Corresponding author: ophir.klein@ucsf.edu – +1-415-476-4719.

Introduction

Abnormalities of the external genitalia are among the most common birth defects in humans. Hypospadias is a condition in which the urethral meatus is abnormally placed along the ventral side of the penis rather than at the distal tip. It affects approximately 1 in every 250–300 live male births, and in spite of the best efforts at surgical reconstruction, it can result in severe psycho-sexual problems and voiding abnormalities (Paulozzi et al., 1997). Studies of patients with hypospadias have identified rare mutations in several genes (Chen et al., 2007; Fukami et al., 2006; Silver and Russell, 1999), but the majority of cases remain idiopathic. Despite the high incidence of congenital anomalies affecting the external genitalia, the molecular mechanisms that control its development are not completely understood.

Development of the external genitalia in humans begins around 4 weeks of gestation, when mesenchymal cells migrate to and cluster at the border of the cloacal membrane. These cells form the genital tubercle (GT), which is the anlage of the male glans penis and female glans clitoridis. Appearance of the GT is accompanied by formation of paired genital swellings flanking the cloacal membrane. Shortly thereafter, urogenital folds are formed along the lateral edges of the cloacal membrane. Up until week 12, the male and female external genitalia are indistinguishable. Subsequent differentiation of male genitalia is hormone-driven. Androgens act on the genital tissues to induce outgrowth of the GT, remodeling of the urogenital folds into a penis with an internalized urethra, and fusion of the genital swellings to form the scrotum (Baskin, 2004; Cunha and Baskin, 2004).

GT morphogenesis in mice closely parallels that in humans (Figure 1). Initiation of GT formation occurs around embryonic day (E) 10.5 with the emergence of bilaterally paired genital swellings composed of mesenchyme and overlying ectoderm encompassing an endoderm-derived epithelium. The genital swellings fuse into a single GT by E11.75. An endoderm-derived urethral plate epithelium spans the proximo-distal axis of the GT along the midline. Preputial swellings, which give rise to the prepuce, appear lateral to the GT at E13.5. By E16.5, the preputial swellings have fused at the ventral midline of the tubercle, enclosing the urethral plate epithelium and forming the internalized tubular urethra (Perriton et al., 2002). At this stage, the GT is ambisexual and the male organ is indistinguishable from the female.

A network of signaling molecules and transcription factors mediates the epithelial-mesenchymal interactions that pattern the GT. The distal urethral epithelium (DUE) directs outgrowth and patterning of the GT by acting as a primary signaling center, similar to the apical ectodermal ridge of the developing limb. Removal of the DUE results in reduced outgrowth of the embryonic GT and downregulation of mesenchymal *Fgf10*, an important morphogen during GT development (Haraguchi et al., 2000; Ogino et al., 2001; Satoh et al., 2004). Previous studies have identified several genes expressed in the urethral epithelium (urothelium) that promote growth and differentiation of the GT. For example, Sonic hedgehog (*Shh*) regulates expression of several signaling molecules and transcription factors in the surrounding mesenchyme, including *Fgf10*, *Bmp4*, *Wnt5a*, *Nog*, *Msx2*, *Hoxa13* and *Hoxd13* (Lin et al., 2009). Altered expression of any of these mesenchymal factors disrupts crucial processes such as cell proliferation, apoptosis, and responsiveness to extracellular molecular signals, ultimately leading to abnormal formation of the GT (Haraguchi et al., 2000; Lin et al., 2009; Morgan et al., 2003; Satoh et al., 2004; Suzuki et al., 2003; Warot et al., 1997; Yamaguchi et al., 1999).

The Fibroblast Growth Factor (FGF) family of secreted ligands plays a particularly important role in epithelial-mesenchymal interactions during GT morphogenesis. Deletion of either *Fgf10* from the GT mesenchyme or its cognate receptor *Fgfr2-IIIb* from the

urothelium results in an ectopic opening along the ventral surface of the GT at a time when the preputial folds should normally have fused to enclose the urethra (Haraguchi et al., 2000; Satoh et al., 2004). Decreased FGF signaling impairs cell proliferation in the GT, affects organization of the urethral plate epithelium, and reduces the expression of *Shh* in the epithelium (Petiot et al., 2005).

Based on its expression in the DUE, it was initially thought that *Fgf8* was responsible for GT outgrowth and patterning. However, while *Fgf8* is strongly expressed in the DUE at the earliest stages of GT outgrowth, deletion of *Fgf8* from the DUE did not appear to have any adverse effects on the genitalia (Haraguchi et al., 2000; Seifert et al., 2009b). Interestingly, ectopic expression of *Fgf8* led to overproliferation of cells in the GT and aberrant morphology during embryogenesis, suggesting that excessive amounts of FGF can also cause genital defects (Lin et al., 2013). Despite its strong expression during GT outgrowth, the lack of phenotypic defects in *Fgf8*-null mice suggests that redundancy of FGF signals in the GT may be important. This has recently been shown to be the case for FGF receptors present in the developing GT. Deletion of both *Fgfr1* and *Fgfr2* from the urethral epithelium resulted in abnormal maturation of the urethral epithelium, while ablation of FGF signaling in the GT mesenchyme led to significantly decreased outgrowth. These results show that FGF signals control different developmental processes in the urethral epithelium as opposed to the surrounding GT mesenchyme (Lin et al., 2013).

Sprouty genes are intracellular inhibitors of FGF-activated receptor tyrosine kinase (RTK) signaling. First discovered in a screen for mutations affecting *Drosophila* tracheal branching, Sprouty genes have since been shown to be involved in the development of several organs via modulation of RTK signaling induced by FGF, EGF, or GDNF (Basson et al., 2005; Chi et al., 2006; Chi et al., 2004; Hacohen et al., 1998; Klein et al., 2006; Mahoney Rogers et al., 2011; Mailleux et al., 2001; Minowada et al., 1999; Shim et al., 2005). The function of Sprouty genes as inhibitors of FGF signaling led us to hypothesize that they function in GT development. We found that the combined deletion of *Spry1* and *Spry2* in the male mouse embryo profoundly affected genital morphogenesis. Our results show that Sprouty genes are critical regulators of FGF signaling during embryonic patterning of the male GT and are necessary for the normal development of the urethral epithelium and formation of the tubular urethra.

Materials and methods

Mouse maintenance and treatment

All mouse studies were carried out under an approved protocol in strict accordance with the policies and procedures established by the University of California, San Francisco (UCSF) Institutional Animal Care and Use Committee (protocol AN084146). Mice were maintained in a temperature-controlled facility with access to food and water *ad libitum.* *Spry1*$^{-/-}$, *Spry2*$^{-/-}$, and *Fgf10*$^{-/-}$ mutant mouse alleles have been described previously (Basson et al., 2005; Min et al., 1998; Shim et al., 2005). *Spry1*$^{-/-}$*;Spry2*$^{-/-}$ double knockout embryos were generated by breeding male mice homozygous for the p-Actin-Cre transgene and heterozygous for both *Spry1 and Spry2 (β-Actin-Cre*$^{Tg/Tg}$ *;Spry1*$^{+/-}$*;Spry2*$^{+/-}$) to female mice homozygous for floxed alleles of both *Spry1* and *Spry2 (Spry1*$^{fl/fl}$*;Spry2*$^{fl/fl}$) (Petersen et al., 2011). To generate embryos at specific timepoints, adult mice were mated overnight and females were checked for a vaginal plug in the morning. The presence of a vaginal plug was designated E0.5. For cell proliferation assays, pregnant female mice were administered a 100 μL dose of BrdU (10 mg/mL) via intraperitoneal injection. Mice were then sacrificed 2 hours after injection.

Quantitative real-time PCR

Total RNA was isolated from E14.5 male lungs, kidneys, and GTs using Trizol, and 500ng from each sample was used to synthesize cDNA (M-MLV RT; Promega; Madison, WI). Quantification of *Spry1, Spry2, Spry4, Etv4,* and *Etv5* was performed using SsoAdvanced SYBR Green Supermix (Bio-rad; Hercules, CA) carried out in a Biorad C1000 Touch thermal cycler attached to a CFX96 Realtime optical detection module. *Rpl19* (60S ribosomal protein L19) was used to normalize gene expression levels. Three to four biological samples were used to quantify transcript levels for each gene, and each reaction was run in triplicate. The Student's T-test was used to determine whether changes in *Etv4* and *Etv5* gene expression between control and Sprouty mutants were significant.

Histology and 3D reconstruction

GT samples were fixed in 4% paraformaldehyde overnight at 4° C and processed for paraffin sections. 7 μm paraffin sections were cut and stained with hematoxylin and eosin for histological analysis. For 3-dimensional reconstruction of control and mutant GTs, brightfield images of stained serial GT sections were collected using a Leica DM5000B upright microscope connected to a Leica DFC500 digital camera. Images were then analyzed, annotated, and rendered 3-dimensionally using BioVis3D software (Montevideo, Uruguay).

Scanning electron microscopy

Tissue was fixed in 0.1 M sodium cacodylate buffer, 1% osmium tetroxide in 0.1 M sodium cacodylate, and then dehydrated for scanning electron microscopy (SEM). Specimens were dried in a Tousimis AutoSamdri 815 Critical Point Dryer and scanning electron micrographs were obtained using a Hitachi TM-1000 scanning electron microscope. All SEM was performed at the University of California, Berkeley Electron Microscope Lab.

In situ hybridization and immunohistochemistry

Samples were collected and fixed in 4% paraformaldehyde overnight at 4° C, immersed in 30% sucrose/PBS overnight at 4° C, and embedded in O.C.T. compound (Sakura Finetek, Torrance, CA). 10 μm frozen sections were cut using a Microm 550 cryostat and hybridized to DIG-labeled RNA probes for *in situ* detection of RNA transcripts. Sections were treated with 10 μg/mL of proteinase K and acetylated prior to hybridization with probe. DIG-labeled RNA probes were synthesized from plasmids containing full-length cDNA or fragments of *Spry1, Spry2, Spry4, Fgf10, Fgfr1, Fgfr2, Etv4, Etv5, Aldh1a2, Shh, Bmp4,* and *Wnt5a*.

Cell proliferation was assessed using immunohistochemical detection of BrdU on paraffin sections using a rat monoclonal antibody specific for BrdU (Abcam, Cambridge, MA; ab6326, 1:1000 dilution). Slides were treated with 0.2 N HCl in water prior to applying antibody, and positive cells were visualized by diaminobenzidine (DAB) staining after incubation with an HRP-conjugated secondary antibody. Cell proliferation was quantified in coronal sections of control and mutant GTs by calculating the ratio of BrdU-positive cells to the total number of nuclei in the urethral epithelium as determined by counterstaining with hematoxylin. Proliferation was analyzed in two male embryos of each genotype, and a minimum of five representative BrdU-stained sections from each GT was counted to attain cell counts.

Tissue was prepared for paraffin embedding by ethanol dehydration and xylene treatment, 7 μm paraffin sections were cut on a Microm HM325 microtome. Uroplakin III (Nichirei Bioscience Inc., Tokyo, Japan; 1:1000 dilution) and phospho-MEK1/2 (Cell Signaling

Technology, Danvers, MA; 1:200 dilution) were detected by immunohistochemistry using standard protocols.

Results

Sprouty genes are expressed in the developing GT and reflect active FGF signaling in the urethral epithelium

There are four mammalian Sprouty gene family members in the mouse genome, and these have differing patterns of expression in adult and embryonic tissues. *Spry1*, *Spry2*, and *Spry4* are expressed in a number of developing tissues, including heart, lung, brain, and skeletal muscle, whereas *Spry3* is primarily expressed in the adult testis and brain (Minowada et al., 1999). We first assayed Sprouty gene expression in the embryonic GT using *in situ* hybridization to detect transcripts of *Spry1*, *Spry2*, and *Spry4*. *Spry1* and *Spry2* expression was primarily localized to the urethral epithelium at E14.5 (Figures 2A−C′), a stage at which the GT and urethral plate epithelium undergo significant morphogenetic changes. Faint expression of *Spry1* was also detected in the distal mesenchyme on the dorsal surface of the GT (Figure 2A, A'). Expression of *Spry4* in the GT mesenchyme and urethral epithelium was low (Figure 2C, C′), suggesting that *Spry1* and *Spry2* are the primary Sprouty genes acting in embryonic GT development.

Quantitative real-time PCR was also used to measure levels of Sprouty gene expression in the embryonic male GT. By qPCR, we confirmed that *Spry1* and *Spry2* were expressed at higher levels in the GT compared to *Spry4*, and *Spry2* transcripts were the most abundant, with an approximately 2-fold increase relative to *Spry1* (Figure 2D). Other known Sprouty-expressing tissues were also analyzed by qPCR to determine expression levels relative to the GT. Expression of *Spry1* in the GT was higher than *Spry1* levels in the lung, but less than the kidney. By comparison, *Spry2* expression was higher in the GT relative to both kidney and lung. Finally, *Spry4* expression was low in the lung, kidney, and GT, although levels were comparable between kidney and GT (Supplemental Figure 1).

Sprouty gene products are intracellular inhibitors of FGF signaling that act in the cells in which they are expressed. To determine whether Sprouty expression domains overlap with regions of FGF signaling in the GT, we assayed the expression patterns of *Fgf10*, *Fgfr1*, and *Fgfr2*, all of which are critical for normal urogenital development (Haraguchi et al., 2000; Petiot et al., 2005; Satoh et al., 2004; Lin et al., 2013). In accordance with previous findings, *Fgf10* transcripts were localized to the GT mesenchyme at E14.5, with levels appearing to be highest in the mesenchyme adjacent to the urothelium (Figure 2E, E'). Expression of *Fgfr1* was also largely confined to the mesenchymal compartment of the GT, but the regions of highest expression appeared to be in the distal mesenchyme along the dorsal and ventral GT (Figure 2F, F'). By contrast, expression of *Fgfr2*, the primary receptor for FGF10, overlapped with *Spry1* and *Spry2* expression in the urethral epithelium (Figures 2G, G'). The expression of *Fgfr2* suggests that the urethral epithelium is the primary target for FGF10 protein produced in the surrounding mesenchyme. To identify the regions of active FGF signaling in the GT, we probed for *Etv4* and *Etv5*, two members of the ETS family of transcription factors that are critical downstream effectors of FGF signaling. Expression of both *Etv4* and *Etv5 was* essentially restricted to the urethral epithelium, indicating that this is the primary tissue target for FGF ligands in the developing GT (Figures 2H–I').

Deletion of both *Spry1* and *Spry2* in the urethral epithelium leads to abnormal development of the male mouse GT

To understand the role of Sprouty genes in the development of the GT, we analyzed mice carrying mutations in one or more Sprouty genes. Based on our findings that *Spry1* and

Spry2 were the two predominant Sprouty family members expressed in the urethral epithelium, we examined GT development in embryos lacking *Spry1* (*Spry1*$^{-/-}$), *Spry2* (*Spry2*$^{-/-}$), or both *Spry1* and *Spry2* (*Spry1*$^{-/-}$;*Spry2*$^{-/-}$). No defects of GT development were apparent in embryonic or adult mice lacking a single Sprouty gene (data not shown), but embryos in which both *Spry1* and *Spry2* were deleted showed gross morphological abnormalities in male GT development. At E16.5 in control male embryos, the preputial swellings have encircled the GT by growing ventrally and fusing along the ventral midline, while the more proximal labioscrotal swellings have also fused along the midline to form a continuous scrotum (Figure 3D). In *Spry1*$^{-/-}$;*Spry2*$^{-/-}$ male embryos, fusion of both the preputial and labioscrotal folds was interrupted, resulting in a bifid scrotum and an ectopic opening along the proximal-ventral surface of the GT (red arrow, Figure 3E).

Histological examination of E18.5 Sprouty mutant GTs revealed the complete absence of an internal urethra and preputial space (Figure 3H, asterisk), whereas control GTs contained an internal tubular urethra (Figure 3G). Other features of GT development such as mesenchymal condensation, formation of preputial glands and stroma, and appearance of the epithelium covering the GT mesenchyme remained largely intact. Interestingly, we only observed GT defects in male *Spry1*$^{-/-}$;*Spry2*$^{-/-}$ embryos, whereas GT development in female *Spry1*$^{-/-}$;*Spry2*$^{-/-}$ embryos appeared normal (Supplemental Figures 2). To determine if abnormal GT morphology was present at earlier stages of development, we also analyzed E12.5 and E14.5 *Spry1*$^{-/-}$;*Spry2*$^{-/-}$ embryos and found no observable defects (data not shown, Figures 3A, B). Overall size of the GT in Sprouty mutants also did not appear significantly affected, indicating that Sprouty genes do not play a major role in GT outgrowth.

Absence of an internal urethra has been described in mice carrying mutations in *Bmp7* or *EphB2* as a consequence of incomplete urorectal septation (Dravis et al., 2004; Wu et al., 2009). We therefore investigated whether this was the cause of the ectopic opening in *Spry1*$^{-/-}$;*Spry2*$^{-/-}$ GTs. Histological analysis of sagittal E16.5 embryo sections showed two distinct epithelial-lined sinuses separated by a urorectal septum extending to the base of the GT, indicating that extension of the urorectal septum to the ectoderm was complete (Supplemental Figure 3).

To compare the effects of elevated FGF signaling in Sprouty mutants with mutants in which FGF signaling is decreased, we examined GT development in *Fgf10*$^{-/-}$ embryos. GT defects that resembled those in the Sprouty mutants have previously been characterized in these *Fgf10*$^{-/-}$ embryos (Haraguchi et al., 2000; Satoh et al., 2004), although some notable differences were found. At E14.5, the preputial swellings in *Fgf10*$^{-/-}$ embryos were reduced in size relative to the GT, whereas the proximal opening of the urethra was significantly larger compared to both control and *Spry1*$^{-/-}$;*Spry2*$^{-/-}$ embryos (Figure 3C; yellow arrowhead). The E16.5 GT in *Fgf10*$^{-/-}$ embryos was also considerably smaller than either control or Sprouty mutant GTs, whereas the ectopic opening at the base of the GT did not extend into the scrotal region, indicating that the effects of *Fgf10* deletion were restricted to GT growth and urethral development. Despite these gross morphological differences between *Fgf10*$^{-/-}$ and *Spry1*$^{-/-}$;*Spry2*$^{-/-}$ GTs at earlier stages of embryonic development, organization of *Fgf10*$^{-/-}$ GTs was similar to *Spry1*$^{-/-}$;*Spry2*$^{-/-}$ GTs. Histological analysis of *Fgf10*$^{-/-}$ GTs at E18.5 showed that, while the overall size of the GT was small in comparison to the *Spry1*$^{-/-}$;*Spry2*$^{-/-}$ GT, both mutants lacked an internal urethra. Formation of the surrounding mesenchyme, preputial stroma, and preputial glands was unperturbed (Figure 3H, I). In contrast to the male-specific defect seen in *Spry1*$^{-/-}$;*Spry2*$^{-/-}$ embryos, GT defects were found in both male and female *Fgf10*$^{-/-}$ embryos (data not shown).

Because *Spry1* was also expressed at low levels in the GT mesenchyme, we performed tissue-specific deletion of *Spry1* and *Spry2* to determine whether they regulate GT development through the urethral epithelium, GT mesenchyme, or both. We generated $Shh^{CreEGFP};Spry1^{-/-};Spry2^{-/-}$ embryos to remove Sprouty genes in the endoderm-derived urethral epithelium and $Tbx4^{Cre};Spry1^{-/-};Spry2^{-/-}$ embryos to delete Sprouty genes in the genital mesenchyme (Harfe et al., 2004; Luria et al., 2008). GT development in $Tbx4^{Cre};Spry1^{-/-};Spry2^{-/-}$ embryos was indistinguishable from control embryos, whereas GT morphology in male $Shh^{CreEGFP};Spry1^{-/-};Spry2^{-/-}$ embryos phenocopied the global Sprouty knockout embryos, confirming that *Spry1* and *Spry2* are critically required in the urethral epithelium, but not in the GT mesenchyme, during embryonic morphogenesis of the GT (Supplemental Figure 4).

Deletion of *Spry1* and *Spry2* affects cell proliferation in the urethral epithelium, but expression of urothelial markers is not perturbed

To construct a more detailed picture of how Sprouty gene deletion affected the development of the GT, we generated 3-dimensional renderings of the GT, urethra, and urethral lumen from serial histological sections at E14.5. In control embryos, the urethra runs along the ventral midline of the GT and forms a three-horned tube at the proximal end. The lumen forms in a proximal-to-distal direction, and it has not reached the distal end of the GT at this stage (Figures 4A, A'). The urethra in Sprouty mutant embryos was significantly enlarged at the proximal end and did not form recognizable horns. Moreover, the lumen failed to extend as far into the distal GT as in controls (Figures 4B, B'). By contrast, the urethra in $Fgf10^{-/-}$ GTs was hypoplastic, with a less defined proximal urethra and an ectopic opening at the base of the GT (Figures 4C, C; black arrow). Although the gross morphology of $Spry1^{-/-};Spry2^{-/-}$ GTs at E14.5 was not significantly affected, histological analysis revealed abnormal organization of the urothelium. In normal GTs, the urothelium is a 2–3 cell-layered transitional epithelium, with cuboidal or columnar-shaped cells lining the basal lamina and flattened, squamous-like cells lining the urethral lumen (Figure 4D). Compared to controls, the urothelium in $Spry1^{-/-};Spry2^{-/-}$ embryos was thicker, the cells lining the urethral lumen did not form a smooth, flattened surface, and basal cells appeared slightly elongated (Figure 4E). Interestingly, deletion of *Fgf10* had the opposite effect on the urothelium. In $Fgf10^{-/-}$ embryos at E14.5, the urothelium was thin in comparison to controls and was composed of only 1–2 layers of tightly packed cells (Figure 4F).

We examined the fate of the urothelium in late-stage embryos to determine whether deletion of Sprouty genes led to abnormal differentiation or degradation of the epithelium normally lining the urethra. Detection of keratin 14 (K14), an epithelial marker, showed that in control GTs, the urothelium is composed of a basal layer of cuboidal, K14-positive cells and an apical layer of squamous, K14-negative cells (Figure 4G, G', red and black arrowheads). In $Spry1^{-/-};Spry2^{-/-}$ embryos, the epithelium covering the ventral-medial aspect of the GT appeared less differentiated based on its rounded morphology and poor stratification. Nevertheless, positive staining of K14 in the basal cells indicated that the early stages of epithelial differentiation had occurred (Figures 4H, H'). To determine whether terminal differentiation of the urothelium was ultimately affected in Sprouty mutants, we also stained for uroplakin III, a specific marker for differentiated urothelial cells. In control embryos, uroplakin III was expressed on the apical side of cells lining the urethral lumen (Figure 4I). Uroplakin III staining was similarly detected on the apical surface of epithelial cells lining the ventral surface of the $Spry1^{-/-};Spry2^{-/-}$ GTs, indicating that the epithelium retained its urothelial identity even in the absence of both Sprouty genes (Figure 4J).

One important function of FGF signaling is to regulate cell proliferation (reviewed in (Turner and Grose, 2010)). In particular, FGF10 is known to induce proliferation in

urothelial cells and prostate epithelium (Bagai et al., 2002; Thomson and Cunha, 1999), whereas a decrease in cell proliferation was observed in the urothelium of *Fgfr2-IIIb*$^{-/-}$ embryos (Petiot et al., 2005). This led us to ask whether the hyperplasia of the urethral epithelium at E14.5 in *Spry1*$^{-/-}$;*Spry2*$^{-/-}$ embryos was due to elevated levels of cell proliferation. We measured the percentage of proliferating urothelial cells by counting the number of BrdU-positive cells in the urethral epithelium and comparing it to the total number of urothelial cells in multiple coronal sections of the GT at E14.5. Cell proliferation was elevated by approximately 30% in *Spry1*$^{-/-}$;*Spry2*$^{-/-}$ embryos relative to littermate controls (Figure 5A, B, D). Although previous studies have shown that injecting mice with recombinant FGF10 caused an increase in the number of dividing cells in the urothelium, an *in vivo* analysis of proliferation had not been performed in embryos lacking *Fgf10*. Therefore, we quantified the number of BrdU-positive cells in the urethra of *Fgf10*$^{-/-}$ embryos and found that the percentage of cells undergoing cell division was decreased by approximately one-third (Figures 5C, D). Levels of cell death were also measured by TUNEL staining in control and mutant GTs to determine whether changes in apoptosis were responsible for the abnormal urethral development observed in Sprouty and FGF mutants, but no significant differences were found (data not shown). Taken together, these results demonstrate that while the effects of increased or decreased FGF signaling may have opposing effects at the cellular level, they can result in similar morphological defects at the organ level.

Activation of MAPK signaling is elevated in *Spry1*$^{-/-}$;*Spry2*$^{-/-}$ GTs, but other signaling pathways appear unperturbed

Because Sprouty genes are important inhibitors of FGF signaling, we hypothesized that abnormal GT morphology in Sprouty mutant embryos may be a result of aberrant regulation of the FGF pathway. To test this, we examined whether activation of signaling components downstream of the FGF receptor was greater in *Spry1*$^{-/-}$;*Spry2*$^{-/-}$ GTs. We first investigated whether levels of phosphorylated MEK1/2, the activated form of two key MAPK protein kinases, was elevated in Sprouty mutants. In control GTs, cytoplasmic localization of phospho-MEK1/2 was observed throughout the urethral epithelium but was absent in the surrounding genital mesenchyme (Figure 6A). In *Spry1*$^{-/-}$;*Spry2*$^{-/-}$ GTs, phospho-MEK1/2 intensity was markedly increased throughout the epithelium, suggesting that activation of MAPK signaling was increased in the absence of Sprouty genes (Figure 6B).

We next asked if transcriptional regulation of gene targets downstream of FGF signaling was also elevated in Sprouty mutant GTs. *Etv4* and *Etv5*, two members of the ETS family of transcription factors, are downstream targets of FGF signaling whose expression reflects the levels of FGF activity (Kobberup et al., 2007; Liu et al., 2003). Expression of both genes appeared to be greater in the urothelium of *Spry1*$^{-/-}$;*Spry2*$^{-/-}$ E14.5 male GTs compared to controls (Figures 6C–F). Quantification of *Etv4* and *Etv5* RNA transcript levels by qPCR in mutant and control GTs at this stage demonstrated that expression of *Etv4* was significantly increased in *Spry1*$^{-/-}$;*Spry2*$^{-/-}$ male GTs. Although *Etv5* expression also showed a slight increase, our data did not reach statistical significance (Figure 6G). Collectively, these data support the hypothesis that deletion of both *Spry1* and *Spry2* in the GT leads to reduced inhibition of the FGF pathway and abnormal upregulation of MAPK signaling and transcriptional activation of downstream targets.

Initiation, outgrowth, and patterning of the mammalian GT require a number of important signaling molecules and transcription factors, and disruption of these signaling pathways may lead to abnormal formation of the GT. Therefore, we sought to establish whether expression of genes involved in GT development was altered in *Spry1*$^{-/-}$;*Spry2*$^{-/-}$

embryos. One of the central players in genital morphogenesis is the Hedgehog pathway. *Shh* is expressed in the urethral plate epithelium and urothelium throughout embryonic development, and controls the expression of numerous genes in the GT mesenchyme including *Ptc1, Bmp4, Fgf10, Hoxd13, Hoxa13, Nog, Fgf8, Wnt5a*, and *Msx1* (Haraguchi et al., 2007; Lin et al., 2009; Perriton et al., 2002). Deletion of *Shh* early in embryogenesis results in genital agenesis (Haraguchi et al., 2001), and a separate role for *Shh* in urethral formation later in development was found with conditional inactivation of *Shh* after the initiation stage of GT organogenesis (Haraguchi et al., 2007; Lin et al., 2009). Because cell proliferation was reduced in $Shh^{-/-}$ GTs (Haraguchi et al., 2001), we tested whether the elevated levels of proliferation in $Spry1^{-/-};Spry2^{-/-}$ embryos were mediated through increased *Shh* expression. We examined *Shh* expression at E14.5, the first stage at which changes in the urethral epithelium were detected in Sprouty mutant GTs. We found strong expression of *Shh* throughout the urethral epithelium of both control and $Spry1^{-/-};Spry2^{-/-}$ GTs, although levels of *Shh* in Sprouty mutant GTs did not appear significantly elevated compared to controls (Figure 6H, I). These findings were confirmed by quantitative PCR (data not shown). This suggests that deletion of Sprouty genes in the urothelium does not significantly affect levels of *Shh* expression.

Fgf10 expression in the GT is dependent on a feedback loop with *Fgfr2-IIIb* and is also a target of *Shh* (Haraguchi et al., 2001; Petiot et al., 2005), but *Fgf10* expression in the GT mesenchyme of $Spry1^{-/-};Spry2^{-/-}$ embryos was comparable to controls (Figure 6J, K). *Wnt5a* and *Bmp4* are two mesenchymal factors that regulate GT outgrowth and proliferation (Suzuki et al., 2003; Yamaguchi et al., 1999). We investigated whether expression of either of these genes was reduced in $Spry1^{-/-};Spry2^{-/-}$ GTs. In both control and Sprouty mutant GTs, *Wnt5a* transcripts accumulated in the distal mesenchyme of the GT, whereas *Bmp4* expression was evident in the dorsal mesenchyme at the distal tip and along the ventral mesenchyme (Figure 6L–O). These results suggest that FGF signaling is not a major regulator of either Wnt or Bmp signaling in the GT at E14.5. Finally, we asked if Sprouty deletion could lead to changes in retinoic acid signaling, which plays an important role in patterning of the external genitalia (Liu et al., 2011; Ogino et al., 2001). We measured expression of *Aldh1a2*, a gene encoding the enzyme that controls the rate-limiting step in retinoic acid synthesis. Although the region of *Aldh1a2* was somewhat expanded, differences in its expression levels were not obvious between control and mutant embryos (Figures 6P, Q).

Discussion

In mammals, the evolution of external genitalia is a prerequisite for internal fertilization, and abnormal development of the external genitalia presumably lowers reproductive fitness. It is therefore somewhat surprising that in humans, congenital defects of the external genitalia are common. Hypospadias, the most frequent genital anomaly in humans, affects approximately 1 in 250–300 live male births, and reports suggest that its incidence has increased over the last two decades in some populations (Lund et al., 2009; Paulozzi et al., 1997). To date, causal mutations in human patients with hypospadias have only been identified in a few genes, including *SRD5A2, CXorf6, FGF8*, and *FGFR2* (Beleza-Meireles et al., 2007; Kalfa et al., 2008; Ogata et al., 2008; Samtani et al.; Silver and Russell, 1999). However, the majority of these are rare mutations in isolated cases of hypospadias, implying that a considerable number of mutations have yet to be discovered. A better understanding of the molecular mechanisms that control genital development will improve our ability to identify candidate genes involved in genital birth defects.

Here, we present evidence that Sprouty genes are critical modulators of FGF signaling in the embryonic mouse GT and are required for normal development of the external genitalia

during embryogenesis. In the absence of *Spry1* and *Spry2*, male embryos exhibit an ectopic opening along the ventral side of the GT, reflecting an essential component of human hypospadias. Later in gestation, these embryos completely lack an internal tubular urethra, suggesting that the urethral closure defects seen at earlier stages are not simply due to delays in development. Expression of Sprouty genes in the embryonic GT was primarily restricted to the urothelium, which is also the site of *Fgfr2-IIIb* expression. Deletion of *Fgf10, Fgfr2-IIIb*, or *Fgfr1* and *Fgfr2* in combination in the mouse also causes a hypospadias-like phenotype, highlighting the need for functional FGF signaling during GT development (Haraguchi et al., 2000; Petiot et al., 2005; Lin et al., 2013). Expression of Sprouty genes in the urothelium also overlapped with *Etv4* and *Etv5*, two known effectors of FGF signaling, suggesting that urethral defects in $Spry1^{-/-};Spry2^{-/-}$ embryos may be mediated through these two factors. Interestingly, loss of Sprouty function did not appear to affect terminal differentiation of the urothelium, as shown by expression of both K14 and uroplakin III, indicating that failure to form the urethra may not be a result of aberrant epithelial differentiation.

We found that deletion of *Spry1* and *Spry2* led to hyperplasia of the urethral epithelium and increased cell proliferation. Sprouty proteins antagonize FGF-induced RTK signaling by interacting with several downstream components of the Ras/MAPK cascade (Casci et al., 1999; Edwin et al., 2009). One of the primary cellular processes regulated by FGF signaling is proliferation, and changes in the number of cells undergoing division have been reported in many studies in which GT development has been affected (Morgan et al., 2003; Petiot et al., 2005; Seifert et al., 2009a; Suzuki et al., 2003). A major question that has not been resolved from these studies is how changes in cell proliferation translate into the hypospadias phenotype. We found that both increased and decreased levels of FGF signaling affected the organization and thickness of the urothelium. In $Spry1^{-/-};Spry2^{-/-}$ embryos, the urothelium was considerably thicker than controls, whereas in *Fgf10* null embryos, the urothelium was composed of 1–2 layers of seemingly less mature epithelial cells. Recent studies have linked cell proliferation and cell polarity (Bilder, 2004). The urothelium is a polarized epithelium composed of several cell layers that differ in morphology and function. Whether the changes in proliferation in both $Spry1^{-/-};Spry2^{-/-}$ and $Fgf10^{-/-}$ GTs disturb epithelial cell polarity, and ultimately, urethral fusion will need to be explored. Alternatively, changes in cell proliferation may be a secondary effect of disrupted cell polarity caused by aberrant FGF signaling.

It is striking that, in contrast to other mutants displaying similar GT anomalies, the defect in $Spry1^{-/-};Spry2^{-/-}$ embryos only occurs in males and not in females. Hormone-dependent sexual differentiation of the GT is not apparent until E16.5 (Suzuki et al., 2002), suggesting that the sexually dimorphic effects of Sprouty deletion are not a result of differences in androgen or estrogen activity. It is particularly interesting that despite some evidence of being under transcriptional regulation by androgens, mutations in either *Fgf10* or *Fgfr2-IIIb* do not lead to sex differences in GT morphogenesis (Petiot et al., 2005). Therefore, our findings raise the possibility that Sprouty genes represent one of the earliest targets of sexually dimorphic signaling in the developing GT. We were unable to detect any differences in Sprouty gene expression between male and female GTs by *in situ* hybridization (data not shown), but a more detailed exploration of androgen effects on FGF signaling will be required.

The role of Sprouty proteins as inhibitors of FGF signaling was highlighted by our findings that deletion of both *Spry1* and *Spry2* in the embryonic GT led to increased activity of MAPK signaling, as well as increased expression of downstream targets such as *Etv4* and *Etv5*. However, characterization of signaling pathways such as Hedgehog, Bmp, and Wnt in the $Spry1^{-/-};Spry2^{-/-}$ male GT revealed a surprising lack of altered gene expression levels

between controls and mutants. In published reports on GT development in *Fgf10*$^{-/-}$ and *Fgfr2-IIIb*$^{-/-}$ embryos, marked differences in *Shh*, *K14*, and *Bmp4* expression were described (Petiot et al., 2005; Satoh et al., 2004). Therefore, there are likely additional genes that have yet to be identified which are involved in mediating the developmental events studied here. Despite the fact that E12.5 Sprouty mutant male GTs do not appear abnormal, changes in expression of critical genes at early stages of embryogenesis may establish aberrant morphogenetic patterns that later lead to defective development. It is interesting to note that in spite of the large variety of genetic deletions that lead to abnormal GT morphogenesis, many of them produce very similar defects in epithelial fusion along the ventral surface of the GT. This would suggest that internalization of the urethra, as well as formation of a continuous prepuce and scrotum, is highly susceptible to morphological disruption during development. This may also explain why genital defects in humans are such a common occurrence.

Taken as a whole, our findings show that Sprouty genes are necessary to regulate FGF activity in the developing mouse GT. *Spry1*$^{-/-}$;*Spry2*$^{-/-}$ male mice represent a good model for gaining insight into the molecular mechanisms underlying embryonic development of mammalian external genitalia. They also offer a potential entry point for improved understanding of the etiology of congenital defects that affect the external genitalia such as hypospadias. Finally, given the paucity of causal mutations known to induce hypospadias in humans, Sprouty genes are strong candidates for mutation screening in patients with this condition.

Supplementary Material

Refer to Web version on PubMed Central for supplementary material.

Acknowledgments

This work was supported by the National Institutes of Health (R01DK095002, RO1 DK0581050), T32 training grant (5T32DK007790), National Science Foundation (IOS-0920793). This work was also supported in part by a grant from the Urology Care Foundation Research Scholars Program and Amgen, Inc.

References

Bagai S, Rubio E, Cheng JF, Sweet R, Thomas R, Fuchs E, Grady R, Mitchell M, Bassuk JA. Fibroblast growth factor-10 is a mitogen for urothelial cells. J Biol Chem. 2002; 277:23828–37828. [PubMed: 11923311]

Baskin LS. Hypospadias. Adv Exp Med Biol. 2004; 545:3–22. [PubMed: 15086017]

Basson MA, Akbulut S, Watson-Johnson J, Simon R, Carroll TJ, Shakya R, Gross I, Martin GR, Lufkin T, McMahon AP, Wilson PD, Costantini FD, Mason IJ, Licht JD. Sprouty1 is a critical regulator of GDNF/RET- mediated kidney induction. Dev Cell. 2005; 8:229–399. [PubMed: 15691764]

Beleza-Meireles A, Lundberg F, Lagerstedt K, Zhou X, Omrani D, Frisen L, Nordenskjold A. FGFR2, FGF8, FGF10 and BMP7 as candidate genes for hypospadias. Eur J Hum Genet. 2007; 15:405–410. [PubMed: 17264867]

Bilder D. Epithelial polarity and proliferation control: links from the Drosophila neoplastic tumor suppressors. Genes Dev. 2004; 18:1909–2509. [PubMed: 15314019]

Casci T, Vinos J, Freeman M. Sprouty, an intracellular inhibitor of Ras signaling. Cell. 1999; 96:655–655. [PubMed: 10089881]

Chen T, Li Q, Xu J, Ding K, Wang Y, Wang W, Li S, Shen Y. Mutation screening of BMP4, BMP7, HOXA4 and HOXB6 genes in Chinese patients with hypospadias. Eur J Hum Genet. 2007; 15:23–83. [PubMed: 17003840]

Chi L, Itaranta P, Zhang S, Vainio S. Sprouty2 is involved in male sex organogenesis by controlling fibroblast growth factor 9-induced mesonephric cell migration to the developing testis. Endocrinology. 2006; 147:3777–8877. [PubMed: 16675530]

Chi L, Zhang S, Lin Y, Prunskaite-Hyyrylainen R, Vuolteenaho R, Itaranta P, Vainio S. Sprouty proteins regulate ureteric branching by coordinating reciprocal epithelial Wnt11, mesenchymal Gdnf and stromal Fgf7 signalling during kidney development. Development. 2004; 131:3345–5645. [PubMed: 15201220]

Cunha GR, Baskin L. Development of the penile urethra. Adv Exp Med Biol. 2004; 545:87–102. [PubMed: 15086022]

Dravis C, Yokoyama N, Chumley MJ, Cowan CA, Silvany RE, Shay J, Baker LA, Henkemeyer M. Bidirectional signaling mediated by ephrin- B2 and EphB2 controls urorectal development. Dev Biol. 2004; 271:272–902. [PubMed: 15223334]

Edwin F, Anderson K, Ying C, Patel TB. Intermolecular interactions of Sprouty proteins and their implications in development and disease. Mol Pharmacol. 2009; 76:679–919. [PubMed: 19570949]

Fukami M, Wada Y, Miyabayashi K, Nishino I, Hasegawa T, Nordenskjold A, Camerino G, Kretz C, Buj-Bello A, Laporte J, Yamada G, Morohashi K, Ogata T. CXorf6 is a causative gene for hypospadias. Nat Genet. 2006; 38:1369–7169. [PubMed: 17086185]

Hacohen N, Kramer S, Sutherland D, Hiromi Y, Krasnow MA. sprouty encodes a novel antagonist of FGF signaling that patterns apical branching of the Drosophila airways. Cell. 1998; 92:253–633. [PubMed: 9458049]

Haraguchi R, Mo R, Hui C, Motoyama J, Makino S, Shiroishi T, Gaffield W, Yamada G. Unique functions of Sonic hedgehog signaling during external genitalia development. Development. 2001; 128:4241–5041. [PubMed: 11684660]

Haraguchi R, Motoyama J, Sasaki H, Satoh Y, Miyagawa S, Nakagata N, Moon A, Yamada G. Molecular analysis of coordinated bladder and urogenital organ formation by Hedgehog signaling. Development. 2007; 134:525–335. [PubMed: 17202190]

Haraguchi R, Suzuki K, Murakami R, Sakai M, Kamikawa M, Kengaku M, Sekine K, Kawano H, Kato S, Ueno N, Yamada G. Molecular analysis of external genitalia formation: the role of fibroblast growth factor (Fgf) genes during genital tubercle formation. Development. 2000; 127:2471–9471. [PubMed: 10804187]

Harfe BD, Scherz PJ, Nissim S, Tian H, McMahon AP, Tabin CJ. Evidence for an expansion-based temporal Shh gradient in specifying vertebrate digit identities. Cell. 2004; 118:517–287. [PubMed: 15315763]

Kalfa N, Liu B, Klein O, Audran F, Wang MH, Mei C, Sultan C, Baskin LS. Mutations of CXorf6 are associated with a range of severities of hypospadias. Eur J Endocrinol. 2008; 159:453–853. [PubMed: 18635673]

Klein OD, Minowada G, Peterkova R, Kangas A, Yu BD, Lesot H, Peterka M, Jernvall J, Martin GR. Sprouty genes control diastema tooth development via bidirectional antagonism of epithelial-mesenchymal FGF signaling. Dev Cell. 2006; 11:181–901. [PubMed: 16890158]

Kobberup S, Nyeng P, Juhl K, Hutton J, Jensen J. ETS-family genes in pancreatic development. Dev Dyn. 2007; 236:3100–3110. [PubMed: 17907201]

Lin C, Yin Y, Bell SM, Veith GM, Chen H, Huh SH, Ornitz DM, Ma L. Delineating a conserved genetic cassette promoting outgrowth of body appendages. PLoS Genet. 2013; 9:e1003231. [PubMed: 23358455]

Lin C, Yin Y, Veith GM, Fisher AV, Long F, Ma L. Temporal and spatial dissection of Shh signaling in genital tubercle development. Development. 2009; 136:3959–6759. [PubMed: 19906863]

Liu L, Suzuki K, Nakagata N, Mihara K, Matsumaru D, Ogino Y, Yashiro K, Hamada H, Liu Z, Evans SM, Mendelsohn C, Yamada G. Retinoic acid signaling regulates Sonic hedgehog and bone morphogenetic protein signalings during genital tubercle development. Birth Defects Res B Dev Reprod Toxicol. 2011

Liu Y, Jiang H, Crawford HC, Hogan BL. Role for ETS domain transcription factors Pea3/Erm in mouse lung development. Dev Biol. 2003; 261:10–24. [PubMed: 12941618]

Lund L, Engebjerg MC, Pedersen L, Ehrenstein V, Norgaard M, Sorensen HT. Prevalence of hypospadias in Danish boys: a longitudinal study, 1977- 2005. Eur Urol. 2009; 55:1022–6022. [PubMed: 19155122]

Luria V, Krawchuk D, Jessell TM, Laufer E, Kania A. Specification of motor axon trajectory by ephrin-B:EphB signaling: symmetrical control of axonal patterning in the developing limb. Neuron. 2008; 60:1039–5339. [PubMed: 19109910]

Mahoney Rogers AA, Zhang J, Shim K. Sprouty1 and Sprouty2 limit both the size of the otic placode and hindbrain Wnt8a by antagonizing FGF signaling. Dev Biol. 2011

Mailleux AA, Tefft D, Ndiaye D, Itoh N, Thiery JP, Warburton D, Bellusci S. Evidence that SPROUTY2 functions as an inhibitor of mouse embryonic lung growth and morphogenesis. Mech Dev. 2001; 102:81–94. [PubMed: 11287183]

Min H, Danilenko DM, Scully SA, Bolon B, Ring BD, Tarpley JE, DeRose M, Simonet WS. Fgf-10 is required for both limb and lung development and exhibits striking functional similarity to Drosophila branchless. Genes Dev. 1998; 12:3156–6156. [PubMed: 9784490]

Minowada G, Jarvis L, Chi C, Neubuser A, Sun X, Hacohen N, Krasnow M, Martin G. Vertebrate Sprouty genes are induced by FGF signaling and can cause chondrodysplasia when overexpressed. Development. 1999; 126:4465–4475. [PubMed: 10498682]

Morgan EA, Nguyen SB, Scott V, Stadler HS. Loss of Bmp7 and Fgf8 signaling in Hoxa13-mutant mice causes hypospadia. Development. 2003; 130:3095–109. [PubMed: 12783783]

Ogata T, Wada Y, Fukami M. MAMLD1 (CXorf6): a new gene for hypospadias. Sex Dev. 2008; 2:244–504. [PubMed: 18987498]

Ogino Y, Suzuki K, Haraguchi R, Satoh Y, Dolle P, Yamada G. External genitalia formation: role of fibroblast growth factor, retinoic acid signaling, and distal urethral epithelium. Ann N Y Acad Sci. 2001; 948:13–31. [PubMed: 11795391]

Paulozzi LJ, Erickson JD, Jackson RJ. Hypospadias trends in two US surveillance systems. Pediatrics. 1997; 100:831–834. [PubMed: 9346983]

Perriton CL, Powles N, Chiang C, Maconochie MK, Cohn MJ. Sonic hedgehog signaling from the urethral epithelium controls external genital development. Dev Biol. 2002; 247:26–46. [PubMed: 12074550]

Petersen CI, Jheon AH, Mostowfi P, Charles C, Ching S, Thirumangalathu S, Barlow LA, Klein OD. FGF signaling regulates the number of posterior taste papillae by controlling progenitor field size. PLoS Genetics. 2011 In press.

Petiot A, Perriton CL, Dickson C, Cohn MJ. Development of the mammalian urethra is controlled by Fgfr2-IIIb. Development. 2005; 132:2441–5041. [PubMed: 15843416]

Samtani R, Bajpai M, Vashisht K, Ghosh PK, Saraswathy KN. Hypospadias risk and polymorphism in SRD5A2 and CYP17 genes: case-control study among Indian children. J Urol. 185:2334–9334. [PubMed: 21511288]

Satoh Y, Haraguchi R, Wright TJ, Mansour SL, Partanen J, Hajihosseini MK, Eswarakumar VP, Lonai P, Yamada G. Regulation of external genitalia development by concerted actions of FGF ligands and FGF receptors. Anat Embryol (Berl). 2004; 208:479–486. [PubMed: 15340846]

Seifert AW, Bouldin CM, Choi KS, Harfe BD, Cohn MJ. Multiphasic and tissue-specific roles of sonic hedgehog in cloacal septation and external genitalia development. Development. 2009a; 136:3949–3957. [PubMed: 19906862]

Seifert AW, Yamaguchi T, Cohn MJ. Functional and phylogenetic analysis shows that Fgf8 is a marker of genital induction in mammals but is not required for external genital development. Development. 2009b; 136:2643–2651. [PubMed: 19592577]

Shim K, Minowada G, Coling DE, Martin GR. Sprouty2, a mouse deafness gene, regulates cell fate decisions in the auditory sensory epithelium by antagonizing FGF signaling. Dev Cell. 2005; 8:553–564. [PubMed: 15809037]

Silver RI, Russell DW. 5alpha-reductase type 2 mutations are present in some boys with isolated hypospadias. J Urol. 1999; 162:1142–1145. [PubMed: 10458450]

Suzuki K, Bachiller D, Chen YP, Kamikawa M, Ogi H, Haraguchi R, Ogino Y, Minami Y, Mishina Y, Ahn K, Crenshaw EB, Yamada G 3rd. Regulation of outgrowth and apoptosis for the terminal

appendage: external genitalia development by concerted actions of BMP signaling [corrected]. Development. 2003; 130:6209–6220. [PubMed: 14602679]

Suzuki K, Ogino Y, Murakami R, Satoh Y, Bachiller D, Yamada G. Embryonic development of mouse external genitalia: insights into a unique mode of organogenesis. Evol Dev. 2002; 4:133–141. [PubMed: 12004962]

Thomson AA, Cunha GR. Prostatic growth and development are regulated by FGF10. Development. 1999; 126:3693–3701. [PubMed: 10409514]

Turner N, Grose R. Fibroblast growth factor signalling: from development to cancer. Nat Rev Cancer. 2010; 10:116–129. [PubMed: 20094046]

Warot X, Fromental-Ramain C, Fraulob V, Chambon P, Dolle P. Gene dosage-dependent effects of the Hoxa-13 and Hoxd-13 mutations on morphogenesis of the terminal parts of the digestive and urogenital tracts. Development. 1997; 124:4781–4791. [PubMed: 9428414]

Wu X, Ferrara C, Shapiro E, Grishina I. Bmp7 expression and null phenotype in the urogenital system suggest a role in re-organization of the urethral epithelium. Gene Expr Patterns. 2009; 9:224–230. [PubMed: 19159697]

Yamaguchi TP, Bradley A, McMahon AP, Jones S. A Wnt5a pathway underlies outgrowth of multiple structures in the vertebrate embryo. Development. 1999; 126:1211–1223. [PubMed: 10021340]

- Sprouty genes are expressed in the embryonic genital tubercle
- Deletion of both *Spry1* and *Spry2* results in abnormal male genital development
- Levels of cell proliferation are altered in *Spry1*$^{-/-}$;*Spry2*$^{-/-}$ male GTs
- FGF signaling levels are elevated in *SpryT1*$^{-/-}$;*pryT2*$^{-/-}$ male GTs

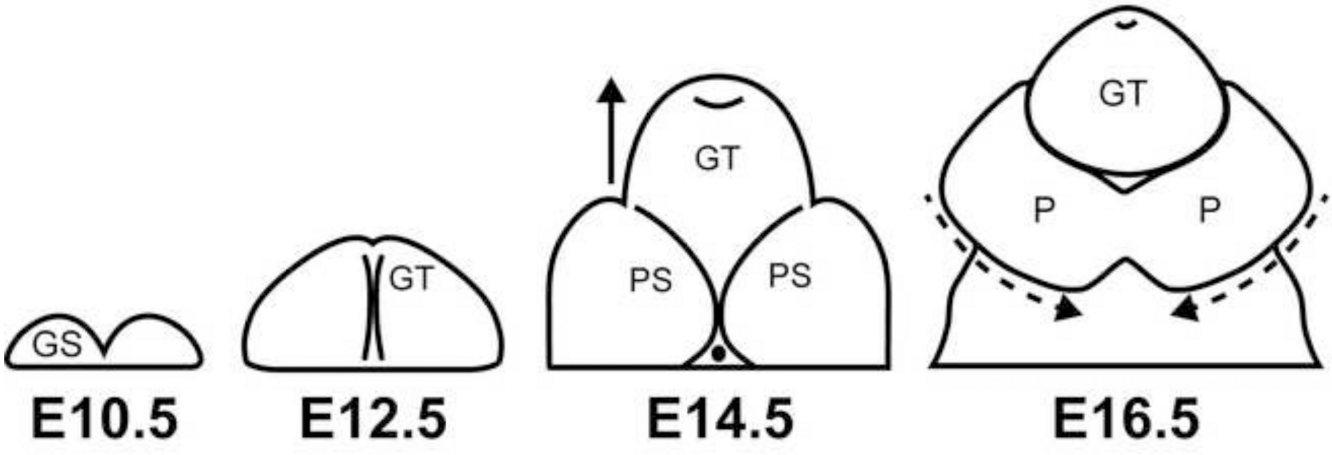

Figure 1. Timeline of mouse external genital development

Cartoons represent a view from the ventral side of the mouse external genitalia during embryonic development. Beginning at E10.5, paired genital swellings (GS) appear. By E12.5, genital swellings have fused to form the genital tubercle (GT). Outgrowth of the GT continues through E14.5 and bilateral preputial swellings (PS) have also appeared. By E16.5, the preputial swellings have fused at the ventral midline to form a continuous prepuce (P) that surrounds the GT.

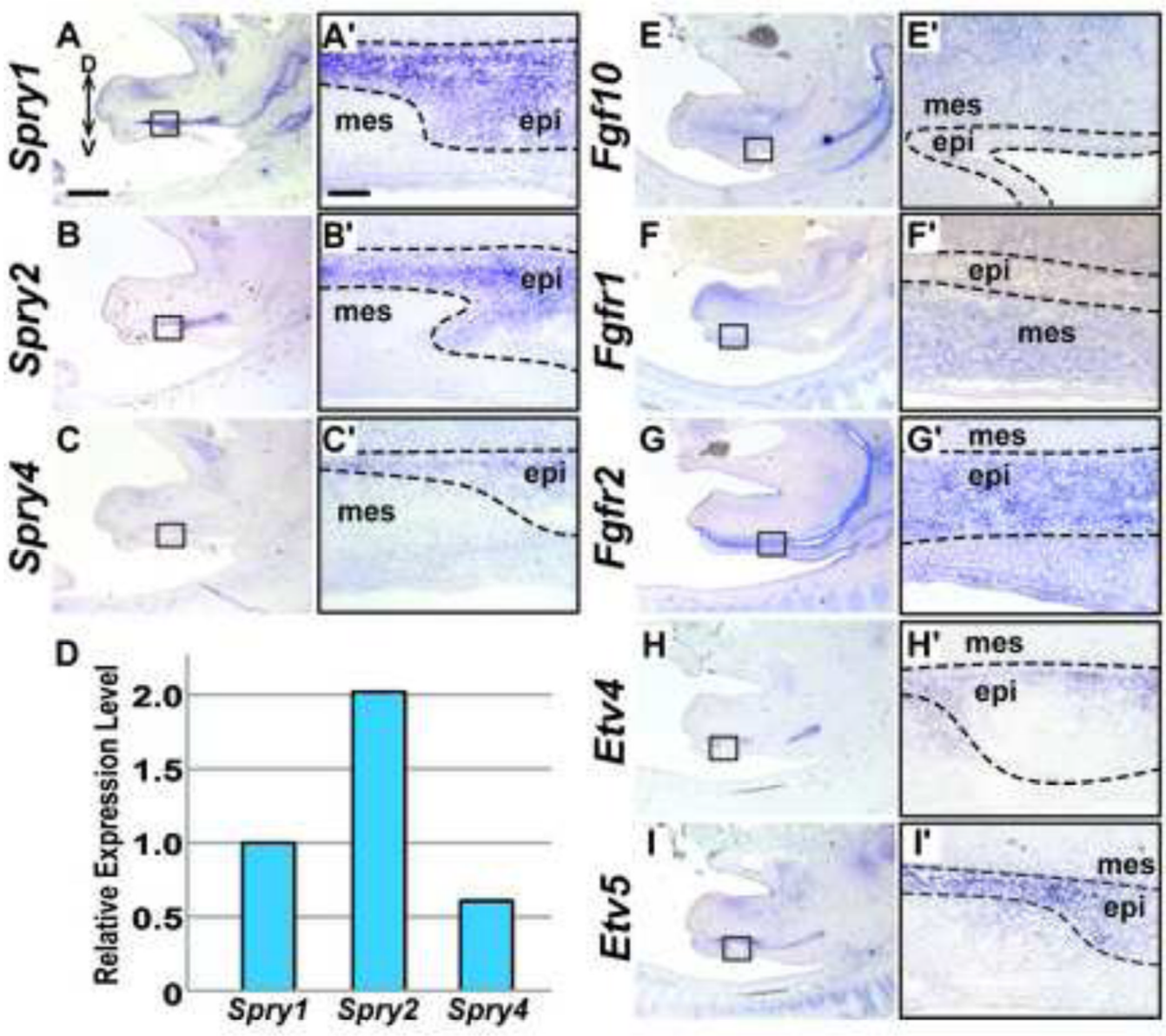

Figure 2. Sprouty and FGF pathway genes are expressed in the embryonic GT

In situ hybridization was used to determine expression patterns of Sprouty and FGF pathway genes in sagittal sections of E14.5 male mouse GTs. *Spry1*, *Spry2*, and *Spry4* mRNA transcripts primarily aggregate in the urethral epithelium, with higher levels of *Spry1* and *Spry2* expression relative to *Spry4* (A-C′). *Spry1*, but not *Spry2*, is detected in a small mesenchymal region on the dorsal region of the distal GT (A, B), while low levels of *Spry4* are diffusely distributed throughout the GT mesenchyme (C). Quantitative PCR detection of *Spry1*, *Spry2*, and *Spry4* transcripts in the male GT at E14.5 show higher expression levels for *Spry1* and *Spry2* in comparison to *Spry4* (D). Both *Fgf10* and *Fgfr1* are expressed in the GT mesenchyme adjacent to the urethral epithelium, while *Fgfr2* expression overlaps with Sprouty in the urothelium (E-G'). *Etv4* and *Etv5* expression is also restricted to the epithelium (H-I'). Black boxes in low-magnification images (A-C, E-I) represent regions shown under high magnification (A'-C′, E'-I'). Urethral epithelium is outlined with black

dots in high-magnification panels (A'- C′, E'-I'). Scale bars, 400 μm (A-C, E-I), 50 μm (A'-C', E'-I'). D, dorsal; V, ventral; epi, epithelium; mes, mesenchyme.

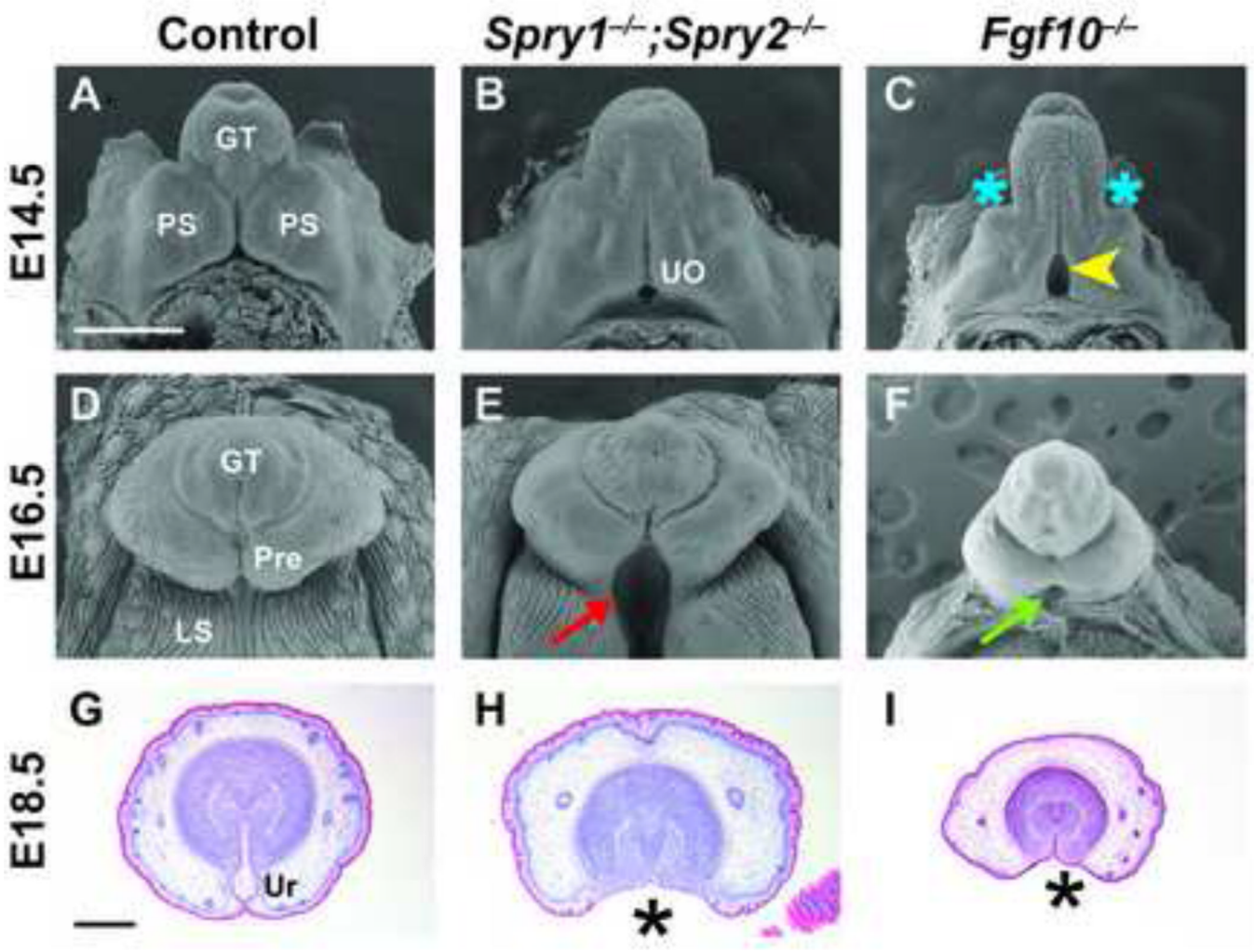

Figure 3. GT development is abnormal in *Spry1*$^{-/-}$;*Spry2*$^{-/-}$ and *Fgf10*$^{-/-}$ embryos

Scanning electron micrographs and histological sections of *Spry1*$^{-/-}$;*Spry2*$^{-/-}$ and *Fgf10*$^{-/-}$ GTs at different stages of development reveal abnormal organogenesis. Gross morphology of the male GT in *Spry1*$^{-/-}$;*Spry2*$^{-/-}$ embryos is similar to controls at E14.5 (A, B). In male E14.5 *Fgf10*$^{-/-}$ embryos, preputial swellings are less prominent (C, blue asterisks) and the urethral meatus appears significantly larger than controls (yellow arrowhead). Fusion of the preputial and labioscrotal folds along the ventral surface of the GT is disrupted in E16.5 male *Spry1*$^{-/-}$;*Spry2*$^{-/-}$ embryos, resulting in the absence of an internalized urethra in the proximal GT (E, red arrow). *Fgf10*$^{-/-}$ GTs are hypoplastic with an ectopic urethral opening at the base of the GT (F, green arrow), but fusion of the labioscrotal folds is not extensively affected. Scale bar, 500 μm. Coronal histological sections of E18.5 control and mutant GTs show that many features of the embryonic GT are preserved in both *Spry1*$^{-/-}$;*Spry2*$^{-/-}$ and *Fgf10*$^{-/-}$ embryos, despite the absence of an internal tubular urethra (G-I, asterisks). Mesenchymal condensations, preputial glands, preputial stroma, and glandular epithelium are not visibly altered (H, I). GT, genital tubercle; PS, preputial swelling; Pre, prepuce; LS, labioscrotal fold; UO, urethral opening; Ur, urethra. Scale bar, 400 μm.

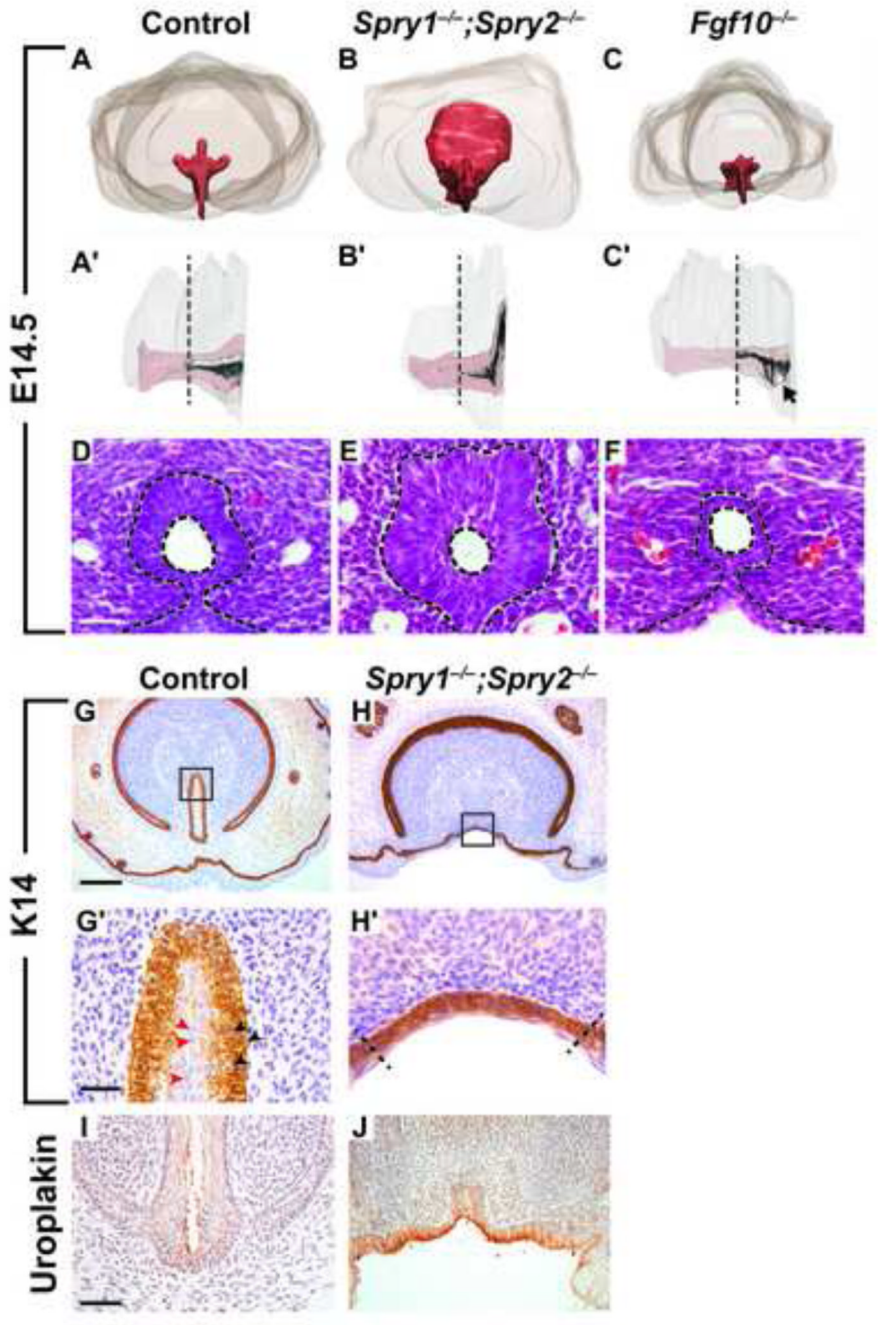

Figure 4. Altered levels of FGF signaling lead to changes in urothelial morphology and structure, but not cell identity

Serial histological sections were used to create 3-dimensional renderings of the GT in control and mutant embryos (A-C′). Coronal view of the urethra (red) in control embryos shows a three-horned structure at the proximal end of the GT (A). A sagittal view shows that the urethral lumen (white) has extended approximately halfway to the distal end of the GT (A'). Both the *Spry1*$^{-/-}$;*Spry2*$^{-/-}$ urethra and urethral lumen are dramatically expanded at the proximal end (B, B'), whereas the urethral epithelium in *Fgf10*$^{-/-}$ GTs is hypoplastic and the proximal urethral opening fails to close (C, black arrow). Black dotted lines in A'-C′ indicate where sections were collected for D-F. Coronal sections of the urethra in E14.5

control and mutant male GTs were stained with hematoxylin and eosin (D-F). In control GTs, the urethral epithelium is composed of a semi-stratified transitional epithelium with columnar cells lining the basal membrane and flattened cells lining the lumen (D). In *Spry1*$^{-/-}$;*Spry2*$^{-/-}$ GTs the urothelium is significantly thicker with few luminal cells exhibiting a squamous morphology (E). The urethral epithelium in *Fgf10*$^{-/-}$ GTs consists of only a thin layer of cuboidal cells (F). Urethral epithelium is outlined in black dotted lines. Scale bar, 30 μm. Characterization of epithelium was done by immunohistochemical staining for K14 (G-H') and uroplakin III (I, J) on coronal sections of E18.5 male control and *Spry1*$^{-/-}$;*Spry2*$^{-/-}$ GTs. Urothelium consists of basal K14-positive cuboidal cells (G'; black arrowheads) and luminal K14-negative squamous cells (G'; red arrowheads). High magnification of K14-stained epithelium in control and *Spry1*$^{-/-}$;*Spry2*$^{-/-}$ GTs (G', H'), dotted lines separate poorly stratified ventral-medial epithelium from lateral epithelium resembling ectoderm-derived epidermis (H'). Scale bars, 200 μm (G, H), 30 μm (G', H'), 50 μm (I, J).

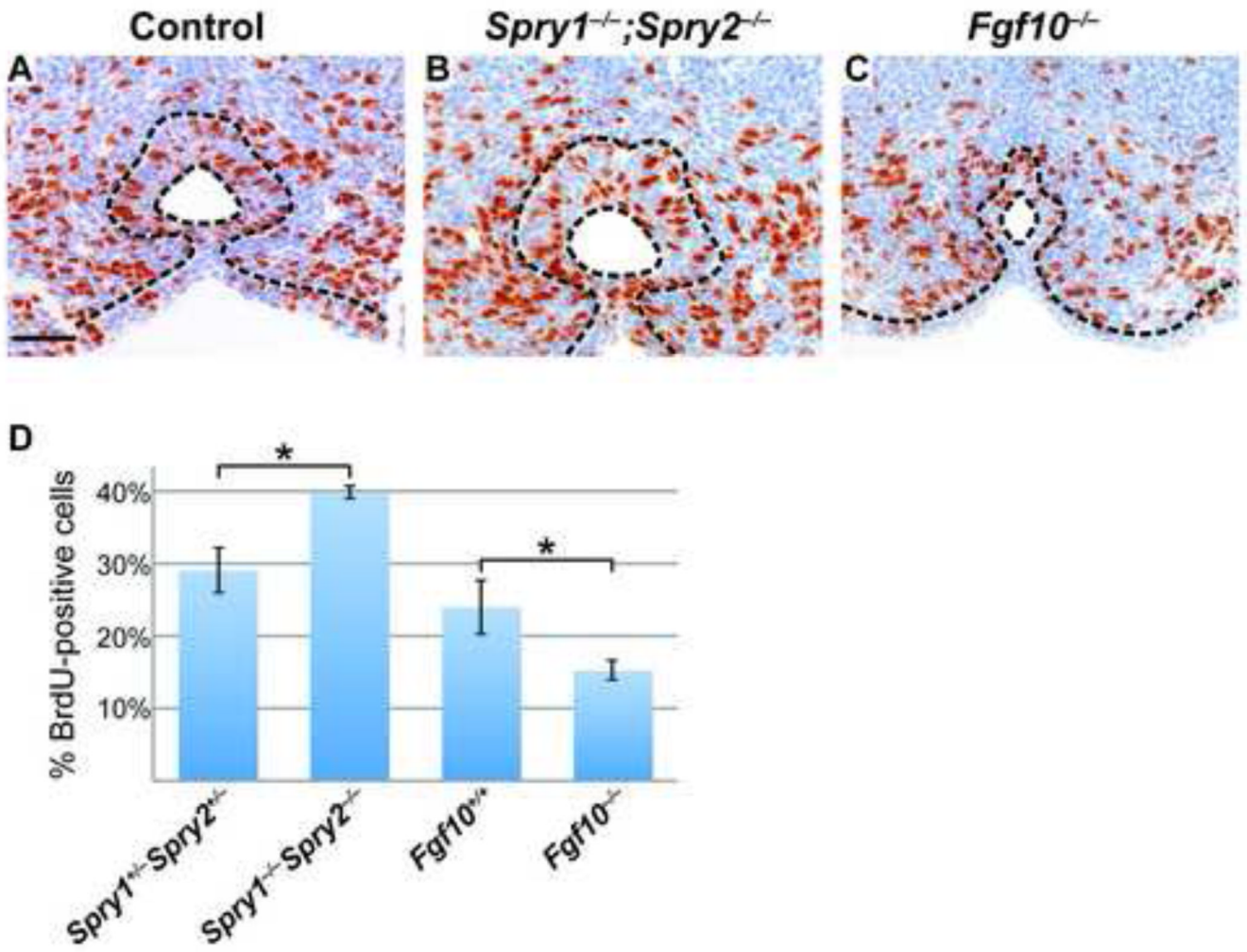

Figure 5. Levels of cell proliferation are affected in *Spry1*$^{-/-}$;*Spry2*$^{-/-}$ and *Fgf10*$^{-/-}$ GTs

Representative coronal sections of E14.5 male GTs from control, *Spry1*$^{-/-}$;*Spry2*$^{-/-}$, and *Fgf10*$^{-/-}$ embryos stained for BrdU (brown) and counterstained with hematoxylin (blue) to visualize cells undergoing proliferation (A-C). Epithelium is outlined in black dotted lines. Scale bar, 50 μm. The proportion of urothelial cells undergoing proliferation was calculated by quantifying the number of BrdU-positive cells and dividing by the total number of epithelial cells. A higher percentage of cells in the urethral epithelium of *Spry1*$^{-/-}$;*Spry2*$^{-/-}$ GTs is undergoing cell division compared to controls, whereas a lower percentage of proliferating cells is seen in the *Fgf10*$^{-/-}$ urethra (D). *, $p < 0.05$.

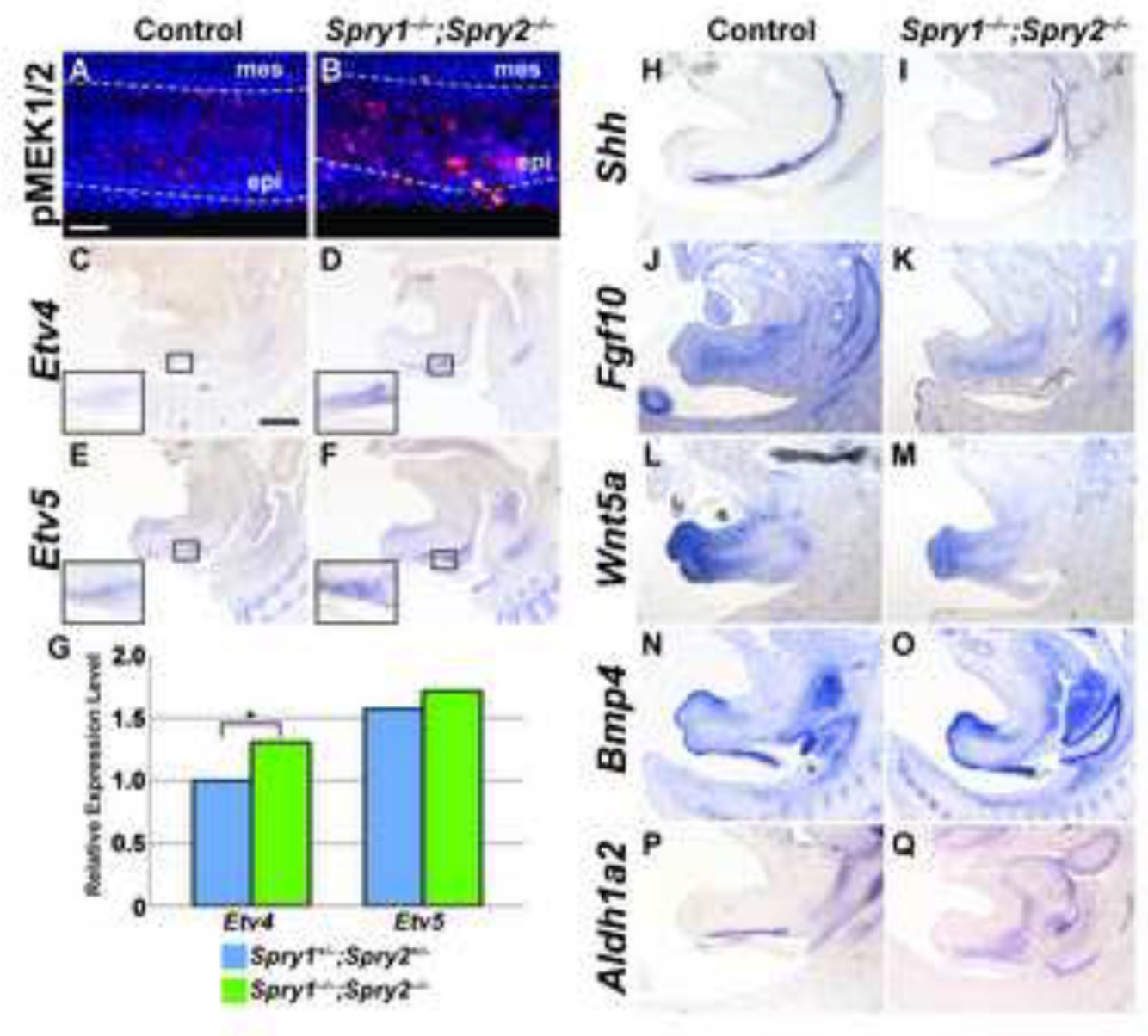

Figure 6. Activation of FGF signaling is increased in *Spry1*$^{-/-}$;*Spry2*$^{-/-}$ GTs, but initiation and maintenance of other signaling pathways is preserved

Levels of MAPK activation in control and Sprouty mutants were assessed by detection of phospho-MEK1/2 in sagittal sections of E14.5 male GTs (A, B). Scale bar, 50μm; epi, epithelium; mes, mesenchyme. *In situ* hybridization was used to examine expression of *Etv4* and *Etv5* in sagittal sections of E14.5 control and *Spry1*$^{-/-}$;*Spry2*$^{-/-}$ GTs. Insets show higher magnification images of the urothelium in control and *Spry1*$^{-/-}$;*Spry2*$^{-/-}$ embryos (C-F). Scale bar, 400 μm. Quantitative real-time PCR detection of *Etv4* and *Etv5* transcript levels showed elevated *Etv4* expression in *Spry1*$^{-/-}$;*Spry2*$^{-/-}$ GTs (G; *, $p < 0.05$). *In situ* hybridization was also used to evaluate expression patterns of *Shh*, *Fgf10*, *Wnt5a*, *Bmp4*, and *Aldh1a2* in E14.5 male control and *Spry1*$^{-/-}$;*Spry2*$^{-/-}$ embryos (H-Q).